

Computer Model Study of the Effect of Resistive Topsoil on Interpretation Results of Subsurface Geoelectric Layers' Parameters.

A.E. Adeniran¹, M.O. Olorunfemi, Ph.D.^{1*}, and O.G. Bayowa²

¹Department of Geology, Obafemi Awolowo University, Ile-Ife, Nigeria.

²Department of Earth Sciences, Ladoké Akintola University, Ogbomosho, Nigeria.

*E-mail: mlorunfe@yahoo.co.uk

ABSTRACT

This paper investigates the effect of resistive topsoil (upper layer) on interpreted subsurface layers' geoelectric parameters. Five hypothetical computer geoelectric models were employed for this study. Model A is a three-layered model with constant thicknesses and varied topsoil resistivity of 100 ohm-m to 2500 ohm-m. Model B is a three-layered model with constant resistivities and varied topsoil thicknesses from 2 to 12 m. Model C is a four-layered model with constant thicknesses and varied topsoil resistivities from 250 to 2500 ohm-m. Model D is a four-layered model with constant thicknesses and varied second layer resistivities from 1000 to 10000 ohm-m. Model E is a four-layered model with constant resistivities and varied second layer thicknesses from 2.0 to 20.0 m.

A total of forty theoretical Vertical Electrical Sounding (VES) curves of the A, H, HA, and KH-type were generated and interpreted using the conventional partial curve matching method and computer assisted 1-D iterative forward modeling with the RESIST 1.0 (Vander-Velpen, 1988) software. Statistical analysis of percentage deviations between model and final interpretation parameters was carried out.

Results obtained from Model A show insignificant overestimated and underestimated second layer geoelectric parameters. Results obtained from Model B show significant overestimated second layer geoelectric parameters - 10.7% to 187.5% and 13% to 204% for percentage resistivity and thickness deviation respectively. Results obtained from Model C show highly overestimated second layer thicknesses and third layer resistivities - 124% to 238% second layer percentage thickness deviation and 96% to 334.7% third layer percentage resistivity deviation. Results obtained from Model D showed highly overestimated third

layer geoelectric parameters – 66.30% to 300.4% and 68% to 316% for percentage resistivity and thickness deviation respectively. Results obtained from Model E show extremely overestimated third layer geoelectric parameters - 183% to 800.7% and 182% to 876% for percentage resistivity and thickness deviation respectively.

The study concludes that the VES technique can yield abnormally high layer parameters for subsurface layers overlain by a resistive topsoil or near surface layer.

(Keywords: resistive topsoil, forward modeling, resistive type curves, curve matching, geoelectric parameters, statistical analysis, vertical electrical sounding, VES)

INTRODUCTION

The electrical resistivity method involving the Vertical Electrical Sounding (VES) technique is extensively used for environmental, groundwater, and engineering geophysical investigations (Zohdy, et al., 1980; Aina, et al., 1996; Olorunfemi, et al., 1993 & 2004; and Afolabi and Olorunfemi, 2004). The success of this technique in the aforementioned depends on the accuracy of the interpretation results of the VES curves in terms of the layer resistivities and thicknesses.

The form of the VES curve is determined by the subsurface layer resistivity combinations and thicknesses. This form is significantly influenced by the resistivity and thickness of the upper layer (topsoil). An increasing topsoil layer resistivity will shift the VES curve vertically upward at small electrode spacings and vertically downward for a decreasing topsoil resistivity. How this shift affects the manifestation of the subsurface layer on the VES curve depends on the resistivity reflection coefficient between the topsoil and the

subsurface layer. Where the reflection coefficient is high (close to ± 1), the subsurface layer may be suppressed and the VES interpretation results will be significantly in error.

This study therefore employs computer modeling to study the effect of thin and thick resistive topsoil (upper layer) on interpreted geoelectrical parameters (thickness and resistivity) of the underlying subsurface layers for common situations encountered in geophysical practice.

Geophysical modeling is the art of studying simplified representations or abstractions of the real earth system based on theoretical laws and principles. It involves defining a system, adopting a significant model, and subjecting the model to thought, test, or simulation. A system is any structure, device, scheme, or procedure, real or abstract, that interrelates in a given time reference, an impact, causes, or stimulus of matter, energy, or information and an output, effect, or response of information, energy or matter (Dooge, 1967). Electrical model studies may involve the generation of electrical responses over regular objects (2D or 3D), which are buried in a medium of contrasting physical properties. Hence, modeling may be conceptual, physical, or mathematical.

In conceptual modeling, processes are imagined in a thought sequence. Physical modeling, also called scale or analog modeling, involves subjection of models to certain test and the mathematical or computer modeling involves simulation of processes using mathematical algorithms. The type adopted in this work is both conceptual and mathematical.

METHODOLOGY

Five hypothetical geoelectric layer models were designed for this study which entailed the calculation, by multi-layer Schlumberger VES forward modeling algorithm, of theoretical (synthetic) curve for each model, the partial curve matching of the curve, and refinement of the interpreted geoelectric parameters using RESIST 1.0 (Vander-Velpen, 1988). Comparison was made between the theoretical and interpreted model results. Ideally, the geoelectric parameters of the theoretical models should be the same as that of the interpreted models.

The Geoelectric Models

Five hypothetical models A, B, C, D, and E (Tables 1 – 5) were employed. For each of the models, one geoelectric parameter was kept constant while the other was gradually increased in a logical sequence.

Geologically, in the basement complex environment models A and B could be simplified models of parallel layers of topsoil with compositional variation from clayey sand to laterite, weathered layer and fresh basement bedrock. In sedimentary area, this could be a simplified model of parallel layers of clayey sand topsoil, sandy clay and sand.

In the basement complex environment, model C could be a simplified geologic model of parallel layers of lateritic topsoil, weathered layer, partially weathered/fractured basement and the fresh basement bedrock while in a sedimentary terrain this could be parallel layers of very sandy topsoil, clay, clayey sand and sand. In the basement complex environment, models D and E could be simplified parallel layers of clay, fresh basement, fractured basement and fresh basement bedrock such that, the fractured basement is sandwiched or confined within the fresh basement rock. In the sedimentary terrain this model could be parallel layers of clay, sand, sandy clay and sand - such that the sandy clay layer is sandwiched between the two sand layers. These models are therefore relevant to both basement complex areas and sedimentary terrains.

Model Characteristics

Model A is a three-layered geoelectric model with constant layer thicknesses but varied topsoil (first layer) resistivities. It is composed of seven sub-models with topsoil resistivity varying from 100 ohm-m to 2500 ohm-m as shown in Table 1.

Model B is a three-layered geoelectric model with constant layer resistivities and varied topsoil (first layer) thicknesses. It is composed of six sub-models with topsoil thicknesses varying from 2 m to 12 m (Table 2).

Model C is a four-layered geoelectric model with constant layer thicknesses and varied topsoil (first layer) resistivities. It is composed of seven sub-models with their corresponding topsoil resistivities varying from 250 ohm-m to 2500 ohm-m (Table 3).

Table 1: Input Geoelectric Parameters for Model A.

| Model | Layer | Starting Model Resistivity (Ohm-m) | Starting Model Thickness (m) |
|-----------|-------|------------------------------------|------------------------------|
| A1 | 1 | 100.00 | 1.50 |
| | 2 | 250.00 | 10.00 |
| | 3 | 100000.00 | - |
| A2 | 1 | 250.00 | 1.50 |
| | 2 | 250.00 | 10.00 |
| | 3 | 100000.00 | - |
| A3 | 1 | 500.00 | 1.50 |
| | 2 | 250.00 | 10.00 |
| | 3 | 100000.00 | - |
| A4 | 1 | 1000.00 | 1.50 |
| | 2 | 250.00 | 10.00 |
| | 3 | 100000.00 | - |
| A5 | 1 | 1500.00 | 1.50 |
| | 2 | 250.00 | 10.00 |
| | 3 | 100000.00 | - |
| A6 | 1 | 2000.00 | 1.50 |
| | 2 | 250.00 | 10.00 |
| | 3 | 100000.00 | - |
| A7 | 1 | 2500.00 | 1.50 |
| | 2 | 250.00 | 10.00 |
| | 3 | 100000.00 | - |

Table 2: Input Geoelectric Parameters for Model B

| Model | Layer | Starting Model Resistivity (Ohm-m) | Starting Model Thickness (m) |
|-----------|-------|------------------------------------|------------------------------|
| B1 | 1 | 2000 | 2 |
| | 2 | 250 | 10 |
| | 3 | 100000 | - |
| B2 | 1 | 2000 | 4 |
| | 2 | 250 | 10 |
| | 3 | 100000 | - |
| B3 | 1 | 2000 | 6 |
| | 2 | 250 | 10 |
| | 3 | 100000 | - |
| B4 | 1 | 2000 | 8 |
| | 2 | 250 | 10 |
| | 3 | 100000 | - |
| B5 | 1 | 2000 | 10 |
| | 2 | 250 | 10 |
| | 3 | 100000 | - |
| B6 | 1 | 2000 | 12 |
| | 2 | 250 | 10 |
| | 3 | 100000 | - |

Table 3: Input Geoelectric Parameters for Model C.

| Model | Layer | Starting Model Resistivity (Ohm-m) | Starting Model Thickness (m) |
|-----------|-------|------------------------------------|------------------------------|
| C1 | 1 | 250.00 | 2.00 |
| | 2 | 100.00 | 5.00 |
| | 3 | 250.00 | 25.00 |
| | 4 | 100000.00 | - |
| C2 | 1 | 500.00 | 2.00 |
| | 2 | 100.00 | 5.00 |
| | 3 | 250.00 | 25.00 |
| | 4 | 100000.00 | - |
| C3 | 1 | 750.00 | 2.00 |
| | 2 | 100.00 | 5.00 |
| | 3 | 250.00 | 25.00 |
| | 4 | 100000.00 | - |
| C4 | 1 | 1000.00 | 2.00 |
| | 2 | 100.00 | 5.00 |
| | 3 | 250.00 | 25.00 |
| | 4 | 100000.00 | - |
| C5 | 1 | 1500.00 | 2.00 |
| | 2 | 100.00 | 5.00 |
| | 3 | 250.00 | 25.00 |
| | 4 | 100000.00 | - |
| C6 | 1 | 2000.00 | 2.00 |
| | 2 | 100.00 | 5.00 |
| | 3 | 250.00 | 25.00 |
| | 4 | 100000.00 | - |
| C7 | 1 | 2500.00 | 2.00 |
| | 2 | 100.00 | 5.00 |
| | 3 | 250.00 | 25.00 |
| | 4 | 100000.00 | - |

Model D is a four-layered geoelectric model with constant layer thicknesses and varied second layer resistivities. It is composed of ten sub-models with their corresponding second layer resistivities varying from 1000 ohm-m to 10000 ohm-m as shown in Table 4.

Model E is a four-layered geoelectric model with constant layer resistivities and varied upper layer thicknesses. It is composed of ten sub-models with their corresponding resistive second layer thicknesses varying from 2 m to 20 m (see Table 5).

Forward Modeling

The theoretical curves (Figures 1–5), with the geoelectric parameters given in Tables 1-5

serving as input, were generated for the forty sub-models by using, BABRES 1.0 Software (Ademilua, 2007 and Ademilua & Olorunfemi, 2008).

Computer Assisted Interpretation

The VES curves were interpreted using the partial curve matching technique with Two Layer Model Curves and the corresponding auxiliary curves (Bhattacharya and Patra, 1968). The geoelectric parameters obtained after partial curve matching were used as initial model parameters for 1-D forward modeling computer-assisted interpretation using the RESIST 1.0 software (Vander-Velpen, 1988). The root-mean-square error in RESIST 1.0 was set to 1%, so that the accuracy of each of the forty sub-models curves

Table 4: Input Geoelectric Parameters for Model D.

| Model | Layer | Starting Model Resistivity (Ohm-m) | Starting Model Thickness (m) |
|--------------|--------------|---|-------------------------------------|
| D1 | 1 | 100.00 | 1.00 |
| | 2 | 1000.00 | 5.00 |
| | 3 | 200.00 | 15.00 |
| | 4 | 100000.00 | - |
| D2 | 1 | 100.00 | 1.00 |
| | 2 | 2000.00 | 5.00 |
| | 3 | 200.00 | 15.00 |
| | 4 | 100000.00 | - |
| D3 | 1 | 100.00 | 1.00 |
| | 2 | 3000.00 | 5.00 |
| | 3 | 200.00 | 15.00 |
| | 4 | 100000.00 | - |
| D4 | 1 | 100.00 | 1.00 |
| | 2 | 4000.00 | 5.00 |
| | 3 | 200.00 | 15.00 |
| | 4 | 100000.00 | - |
| D5 | 1 | 100.00 | 1.00 |
| | 2 | 5000.00 | 5.00 |
| | 3 | 200.00 | 15.00 |
| | 4 | 100000.00 | - |
| D6 | 1 | 100.00 | 1.00 |
| | 2 | 6000.00 | 5.00 |
| | 3 | 200.00 | 15.00 |
| | 4 | 100000.00 | - |
| D7 | 1 | 100.00 | 1.00 |
| | 2 | 7000.00 | 5.00 |
| | 3 | 200.00 | 15.00 |
| | 4 | 100000.00 | - |
| D8 | 1 | 100.00 | 1.00 |
| | 2 | 8000.00 | 5.00 |
| | 3 | 200.00 | 15.00 |
| | 4 | 100000.00 | - |
| D9 | 1 | 100.00 | 1.00 |
| | 2 | 9000.00 | 5.00 |
| | 3 | 200.00 | 15.00 |
| | 4 | 100000.00 | - |
| D10 | 1 | 100.00 | 1.00 |
| | 2 | 10000.00 | 5.00 |
| | 3 | 200.00 | 15.00 |
| | 4 | 100000.00 | - |

Table 5: Input Geoelectric Parameters for Model E.

| Model | Layer | Starting Model Resistivity (Ohm-m) | Starting Model Thickness (m) |
|------------|-------|------------------------------------|------------------------------|
| E1 | 1 | 100.00 | 1.00 |
| | 2 | 5000.00 | 2.00 |
| | 3 | 200.00 | 10.00 |
| | 4 | 100000.00 | - |
| E2 | 1 | 100.00 | 1.00 |
| | 2 | 5000.00 | 4.00 |
| | 3 | 200.00 | 10.00 |
| | 4 | 100000.00 | - |
| E3 | 1 | 100.00 | 1.00 |
| | 2 | 5000.00 | 6.00 |
| | 3 | 200.00 | 10.00 |
| | 4 | 100000.00 | - |
| E4 | 1 | 100.00 | 1.00 |
| | 2 | 5000.00 | 8.00 |
| | 3 | 200.00 | 10.00 |
| | 4 | 100000.00 | - |
| E5 | 1 | 100.00 | 1.00 |
| | 2 | 5000.00 | 10.00 |
| | 3 | 200.00 | 10.00 |
| | 4 | 100000.00 | - |
| E6 | 1 | 100.00 | 1.00 |
| | 2 | 5000.00 | 12.00 |
| | 3 | 200.00 | 10.00 |
| | 4 | 100000.00 | - |
| E7 | 1 | 100.00 | 1.00 |
| | 2 | 5000.00 | 14.00 |
| | 3 | 200.00 | 10.00 |
| | 4 | 100000.00 | - |
| E8 | 1 | 100.00 | 1.00 |
| | 2 | 5000.00 | 16.00 |
| | 3 | 200.00 | 10.00 |
| | 4 | 100000.00 | - |
| E9 | 1 | 100.00 | 1.00 |
| | 2 | 5000.00 | 18.00 |
| | 3 | 200.00 | 10.00 |
| | 4 | 100000.00 | - |
| E10 | 1 | 100.00 | 1.00 |
| | 2 | 5000.00 | 20.00 |
| | 3 | 200.00 | 10.00 |
| | 4 | 100000.00 | - |

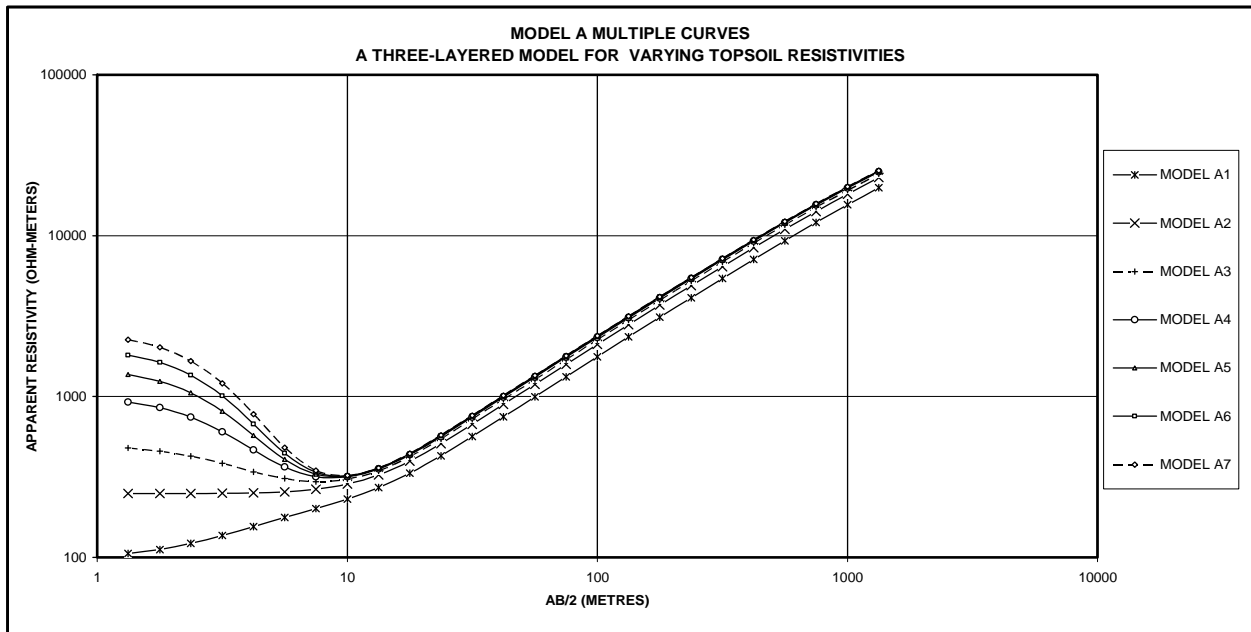


Figure 1: Theoretical VES Curves for Model A.

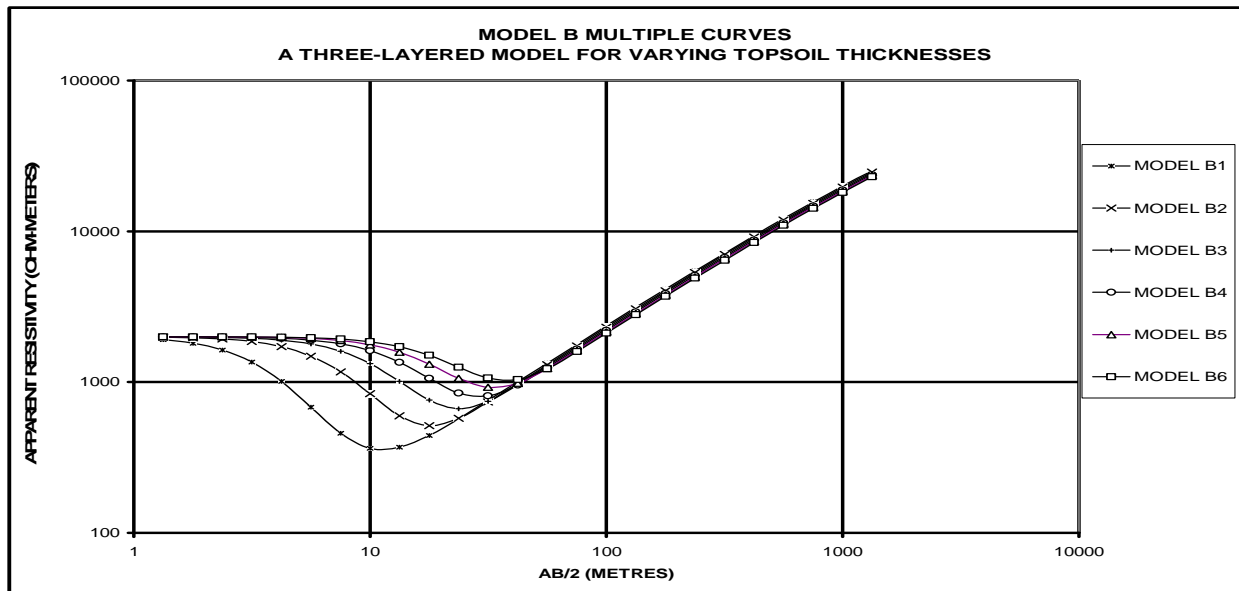


Figure 2: Theoretical VES Curves for Model B.

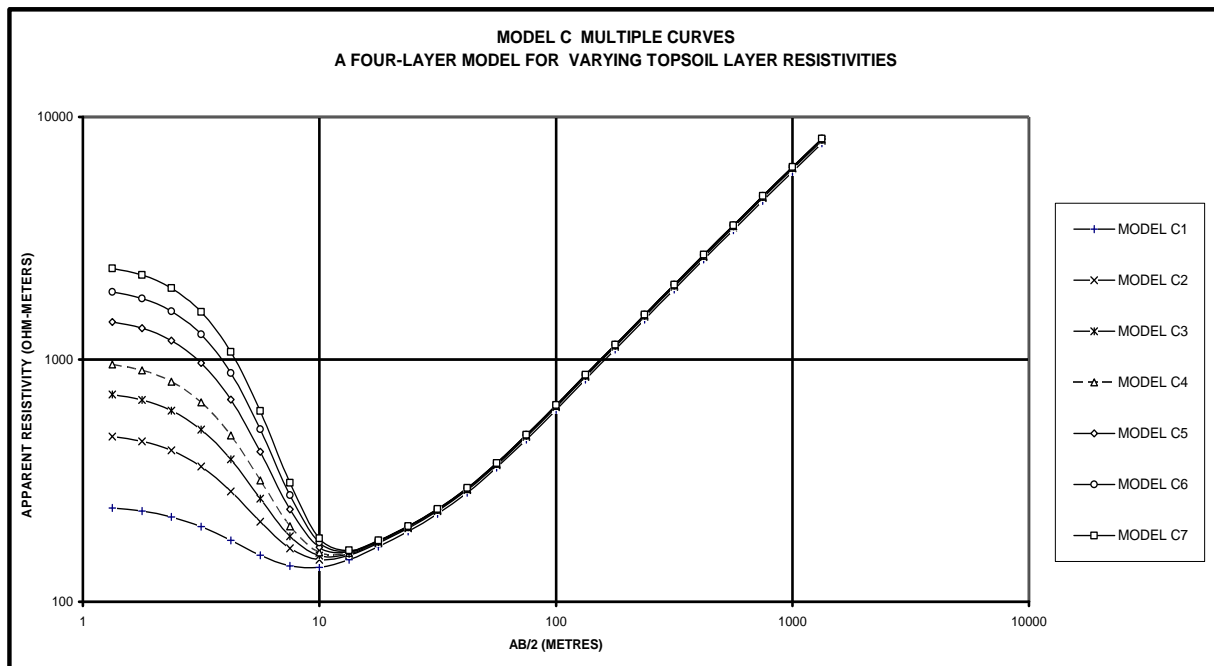


Figure 3: Theoretical VES Curves for Model C.

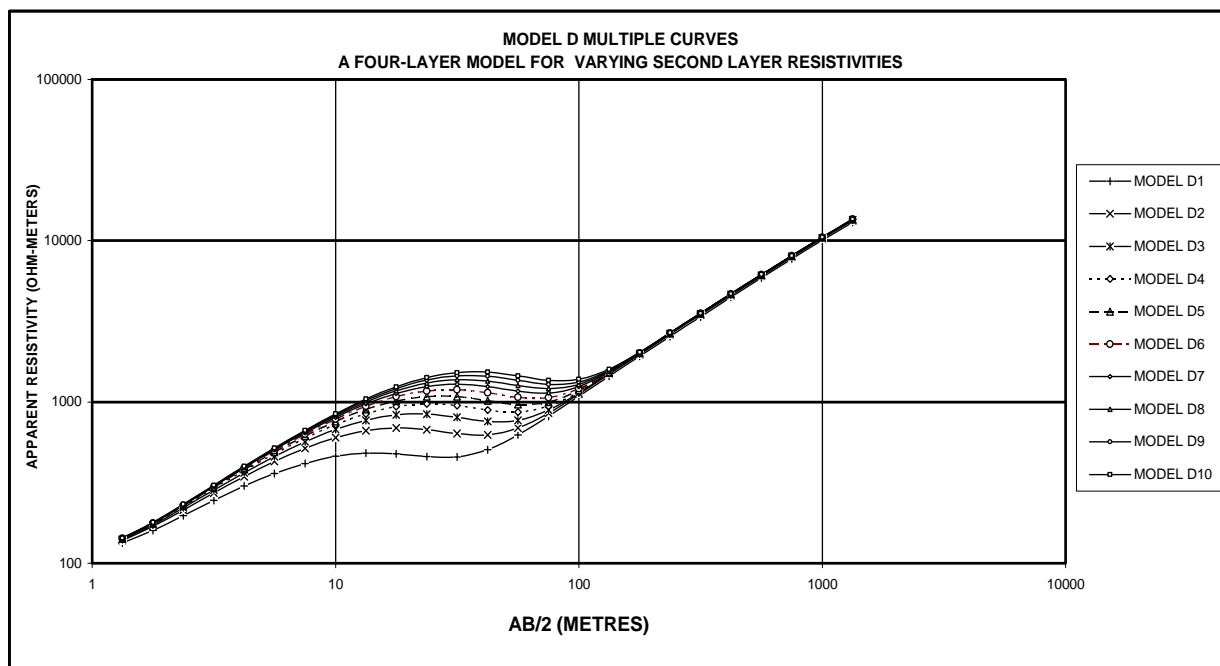


Figure 4: Theoretical VES Curves for Model D.

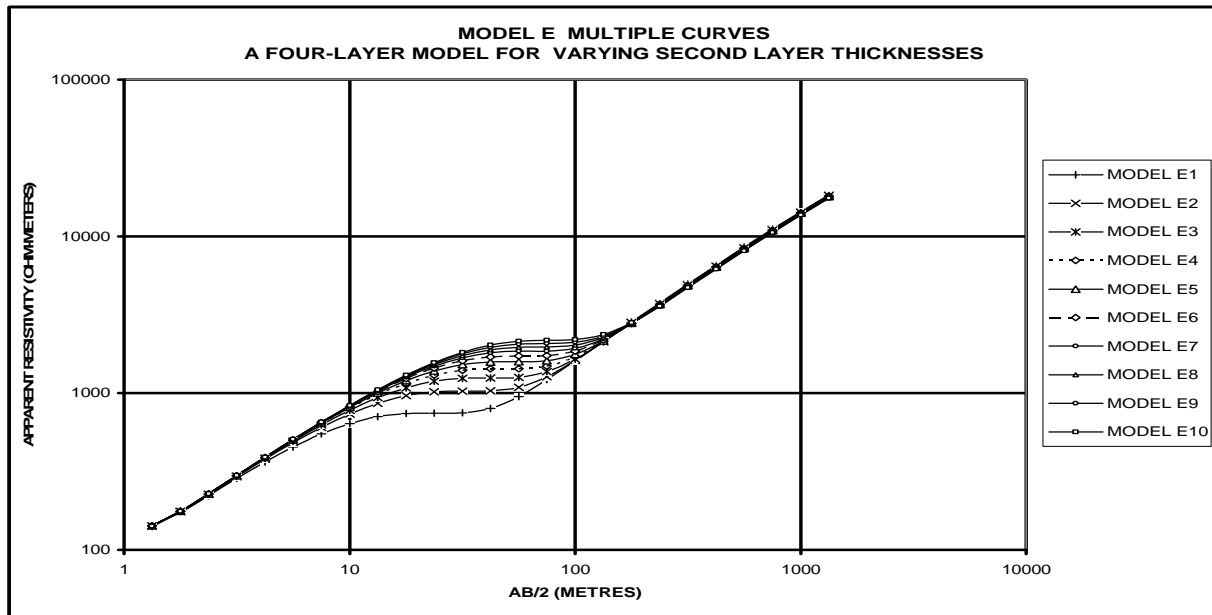


Figure 5: Theoretical VES Curves for Model E.

could be at least 99% since the curves are plots of ideal synthetic data. Examples of the comparison of the theoretical data and interpretation model curves are shown in Figure 6.

Analysis of Interpretation Results

The comparison between the sets of theoretical and interpreted model parameters was carried out based on percentage deviation. The Percentage Deviation, $(PD)_{(GP)}$, in the geoelectric parameters for each sub-model was calculated using the equation:

$$PD_{(GP)} = \left[\frac{GE_{(SM)} - GE_{(IM)}}{GE_{(SM)}} \right] 100 \%$$

where $GE_{(SM)}$ is the theoretical model's geoelectric parameter (thickness or resistivity) and $GE_{(IM)}$ is the interpreted model's geoelectric parameter (thickness or resistivity).

Histograms and frequency curves were generated from the percentage deviations for each of the model groups. The highest point on the graph gives the modal class.

RESULTS AND DISCUSSION

Synthetic Multilayered VES Curves

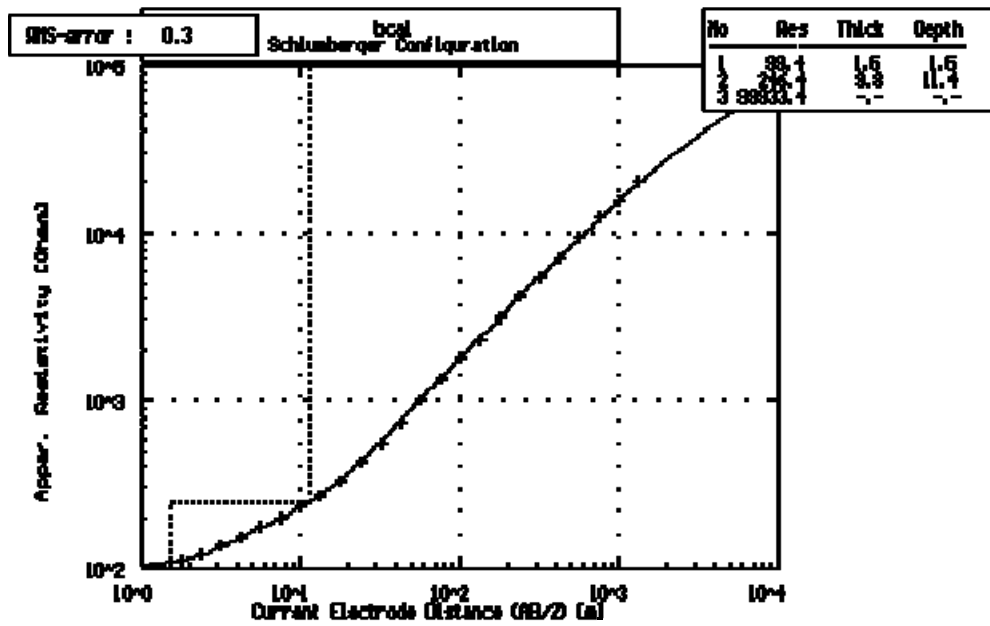
The VES curves generated for model A are the three-layer A-type and H-type curves (Figure 1). Increase in the first layer resistivity shifted the curves vertically upwards at small electrode spacing and transformed it from A type curves to H type curves. The curves show limited vertical shift at large spacing for models A1 to A3, otherwise no significant influence.

The model curves generated from model B are the three-layer H-type curves (Figure 2). Increase in first layer resistivity also shifted the curves vertically upwards at relatively small electrode spacing and make the curves approach asymptotic value. There is virtually no effect at large electrode spacing.

The curves generated from model C are the four layer HA-type curves (Figure 3). Increase in the first layer resistivity shifted the VES curves vertically upwards at small electrode spacing with virtually no influence at large electrode spacing.

The curves generated from model D are the four-layer KH-type curves (Figure 4). Increase in the second layer resistivity led to increase in apparent resistivity values and vertical shift of the curves at

(a)



(b)

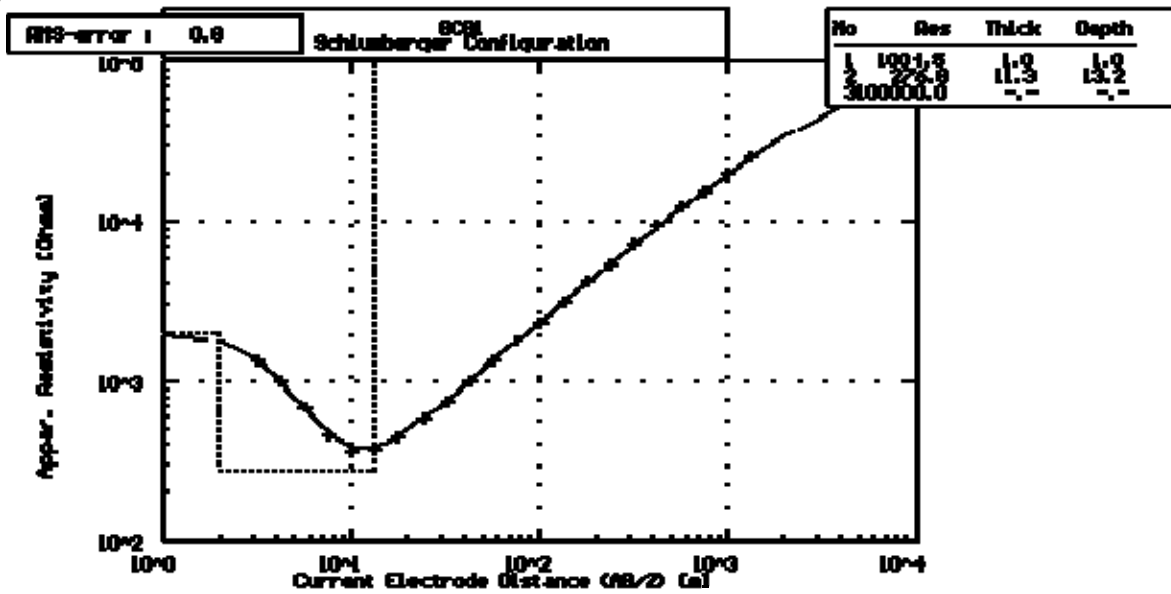


Figure 6: Comparison of Theoretical data and Interpreted Model Curves for Models A1 and B1.

intermediate electrode spacing. The curves are not significantly affected at relatively small and large electrode spacing.

The curves generated from model E are the four layer KH-type curves (Figure 5). Increase in the second layer thickness also led to vertical shift of the curves at intermediate electrode spacing with virtually no influence at relatively small and large electrode spacing.

Histograms

The computed geoelectric parameters' percentage deviations were plotted as histograms (Figures 7a and 7b) for the various models. For model A, the histograms show that the influence of thin resistive first layer on the second layer was insignificant, since all thickness and resistivity percentage deviations are within the range of – 5 % (underestimation) to 6 % (overestimation).

For model B, the histograms show significant overestimation of the second layer's geoelectric parameters (Figures 8a and 8b). The overestimation of the second layer's resistivity ranges from 10.7% to 187.5% while that of the thickness varies from 13.0% to 204.0%.

For model C (Figures 9a, 9b, 10a and 10b), the percentage deviation in the second layer resistivity ranges from 18.2% to 39.7% while the percentage thickness deviation ranges from 124.0% to 238.0%. The effect of the resistive first layer is greater on the thickness of the second layer than the resistivity of the layer. In the third layer the percentage resistivity deviation ranges from 96.6% to 334.7% while the percentage thickness deviation ranges from 8% to 31.6%. The effect of the resistive first layer is greater on the resistivity of the third layer than its thickness.

For model D, the significant overestimation in the third layer percentage resistivity deviations ranges from 66.30% to 300.40% while that of the thickness ranges from 68.00% to 316.7% (Figures 11a and 11b).

For model E (Figures 12a and 12b), the overestimation in the third layer resistivity ranges from 183.0% to 800.7% while that of the thickness ranges from 182.0% to 876.0%.

Frequency Curves

Frequency curve were plotted for each of the affected subsurface layers. The most prevailing percentage geoelectric parameter deviation (for both thickness and resistivity) in model A is -4.0% (Figure 13a), which implies that model A is insignificantly underestimated.

Model B frequency curves show that for the second layer the prevailing percentage thickness deviation (70%) is greater than twice that of the percentage resistivity deviation (30%) (Figure 13b). This implies that the significant overestimation in thickness of the second layer could be twice as large as that of the resistivity for this model.

For model C, the prevailing percentage thickness deviation (150%) in the second layer, could be as large as five times that of the percentage resistivity deviation (27%) (Figure 13c).

The percentage resistivity deviation (115%) in the third layer could be as large as nine times that of the percentage thickness deviation (8-16%) (Figure 13d). The prevailing percentage thickness deviation for this layer shows that the layer's thickness may only be slightly overestimated.

For model D, the prevailing percentage geoelectric deviation is 325% (Figure 13e) (for both thickness and resistivity of the third layer). This implies that the geoelectric parameters (thickness and resistivity) of this model may be significantly overestimated proportionately.

For model E, the prevailing percentage geoelectric deviation is 550% (Figure 13f) (for both thickness and resistivity of the third layer). This implies that the geoelectric parameters (thickness and resistivity) of this model may be highly overestimated proportionately.

CONCLUSIONS

A 1-D computer model study of the effect of thin and thick resistive topsoil on the interpretation of subsurface layers' geoelectric parameters was carried out. Comparative analyses were carried out between the theoretical model geoelectric parameters and the computer aided interpretation model geoelectric parameters of five hypothetical geoelectric models.

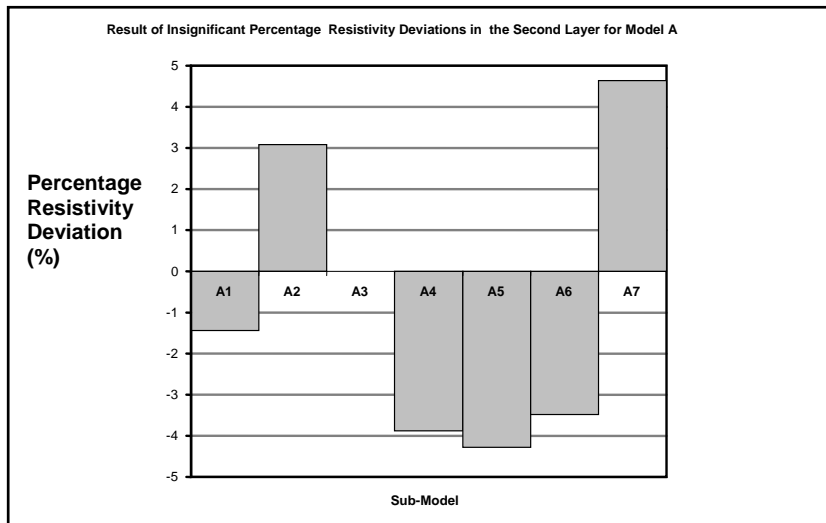


Figure 7(a): Histogram of Percentage Deviation for Second Layer Resistivity for Model A.

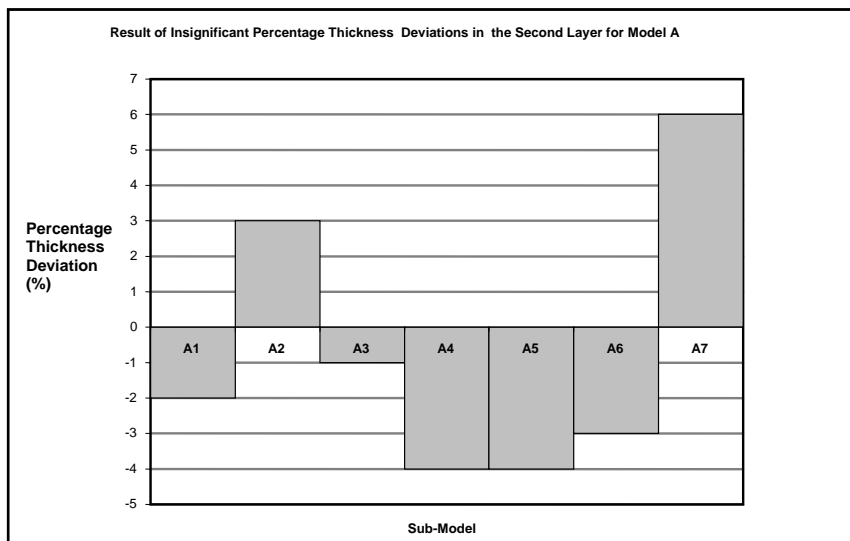


Figure 7(b): Histogram of Percentage Deviation for Second Layer Thickness for Model A.

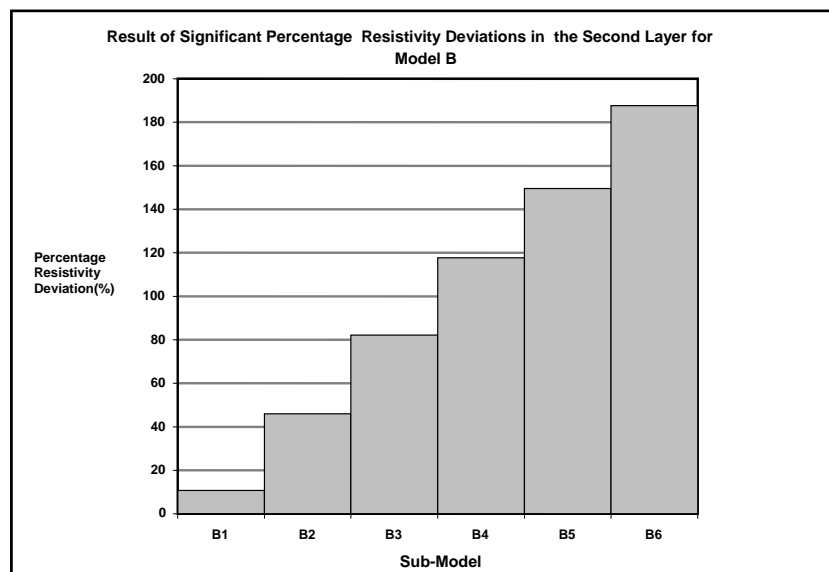


Figure 8(a): Histogram of Percentage Deviation for Second Layer Resistivity for Model B.

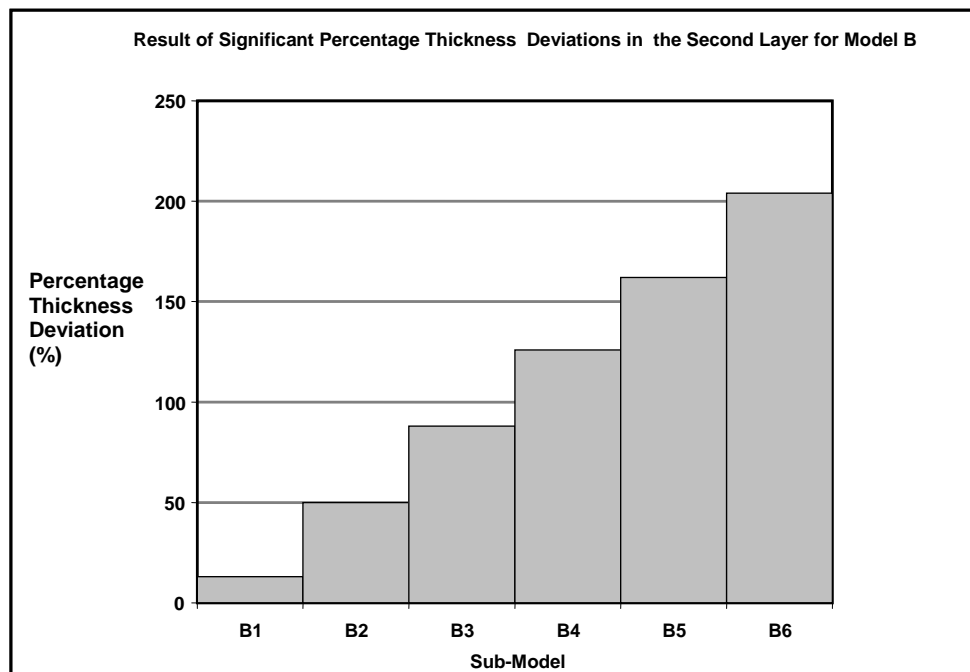


Figure 8(b): Histogram of Percentage Deviation for Second Layer Thickness for Model B.

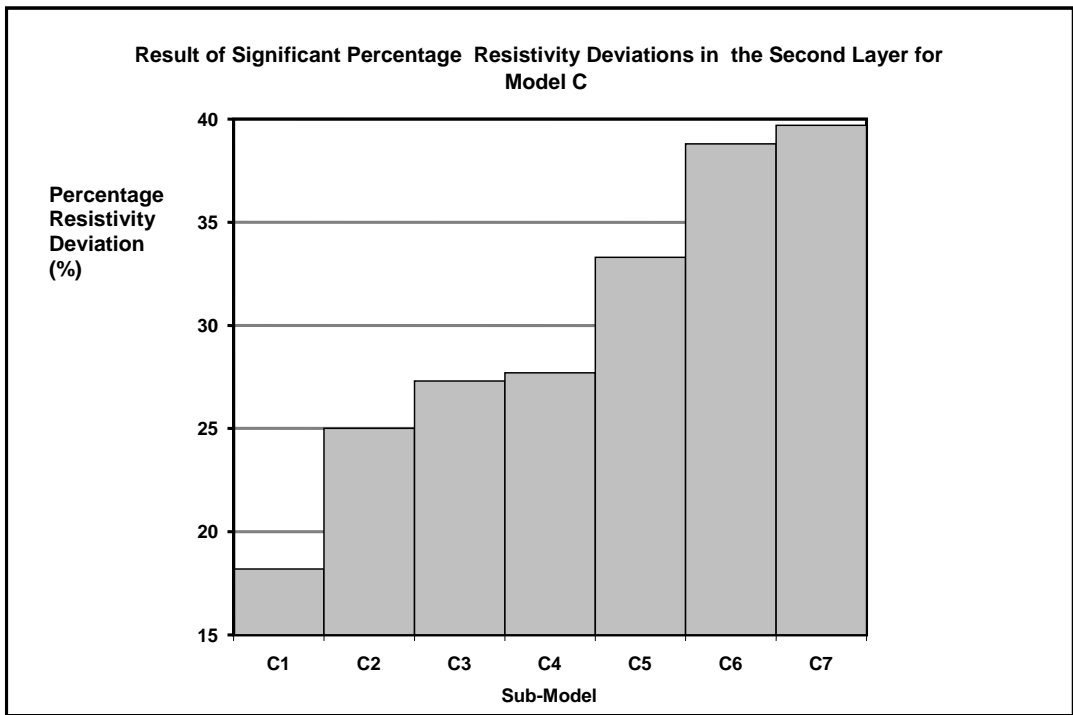


Figure 9(a): Histogram of Percentage Deviation for Second Layer Resistivity for Model C.

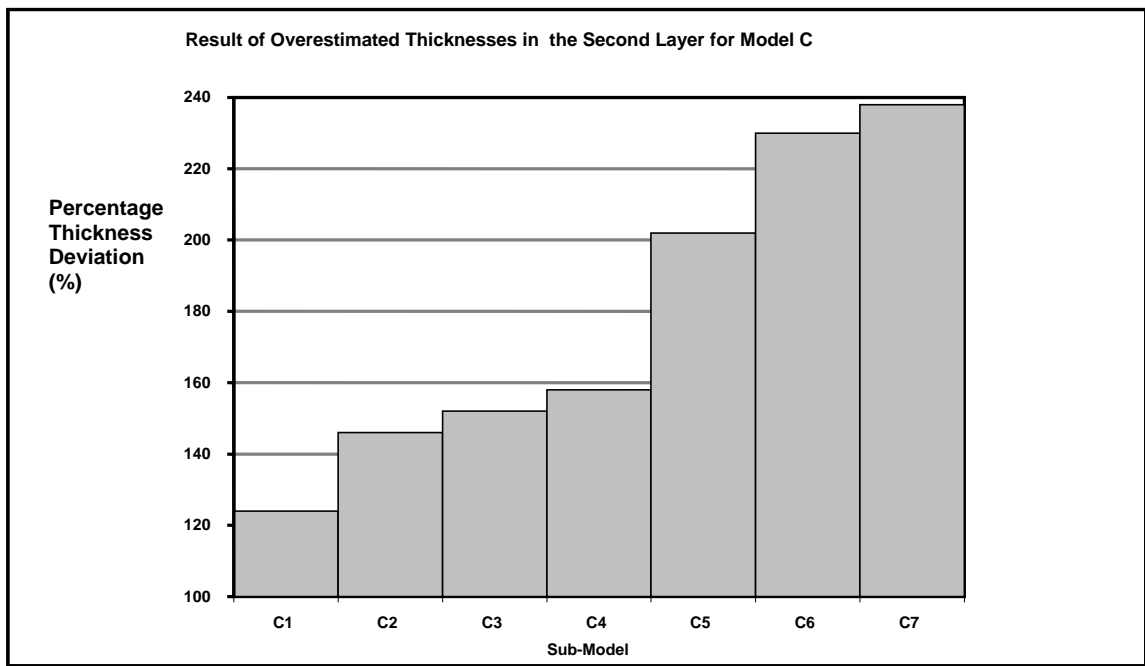


Figure 9(b): Histogram of Percentage Deviation for second Layer Thickness for Model C.

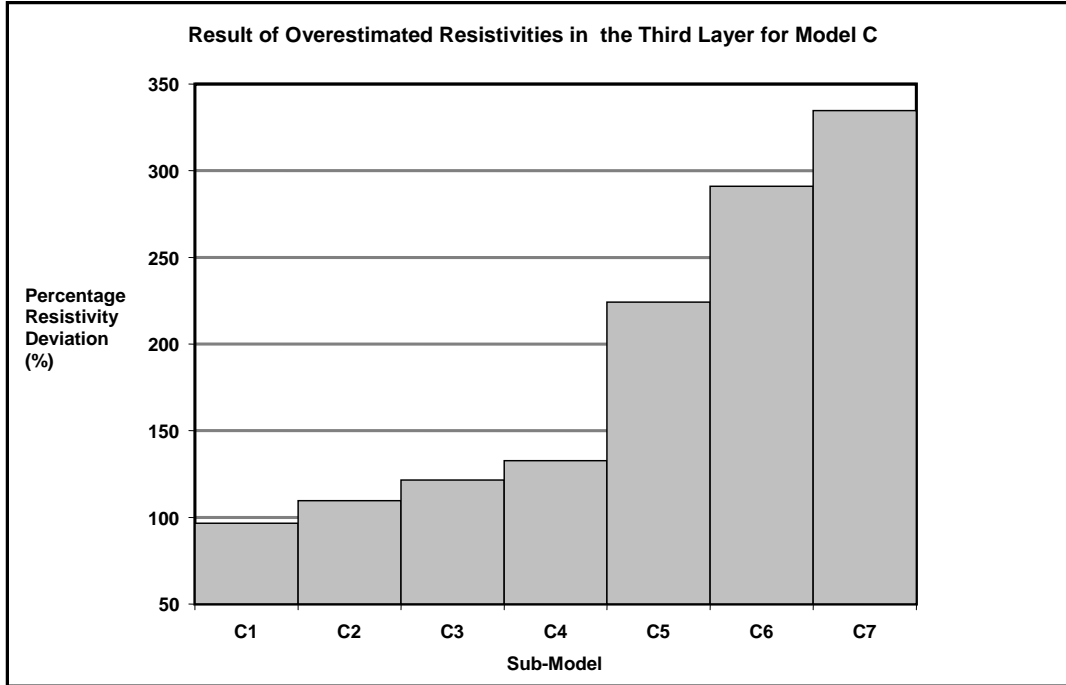


Figure 10(a): Histogram of Percentage Deviation for Third Layer Resistivity for Model C.

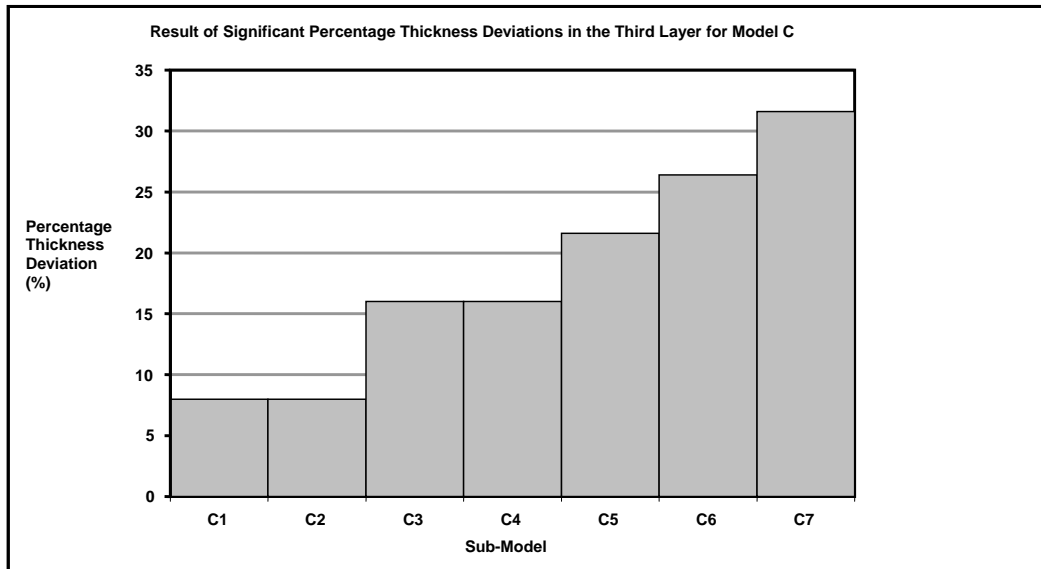


Figure 10(b): Histogram of Percentage Deviation for Third Layer Thickness for Model C.

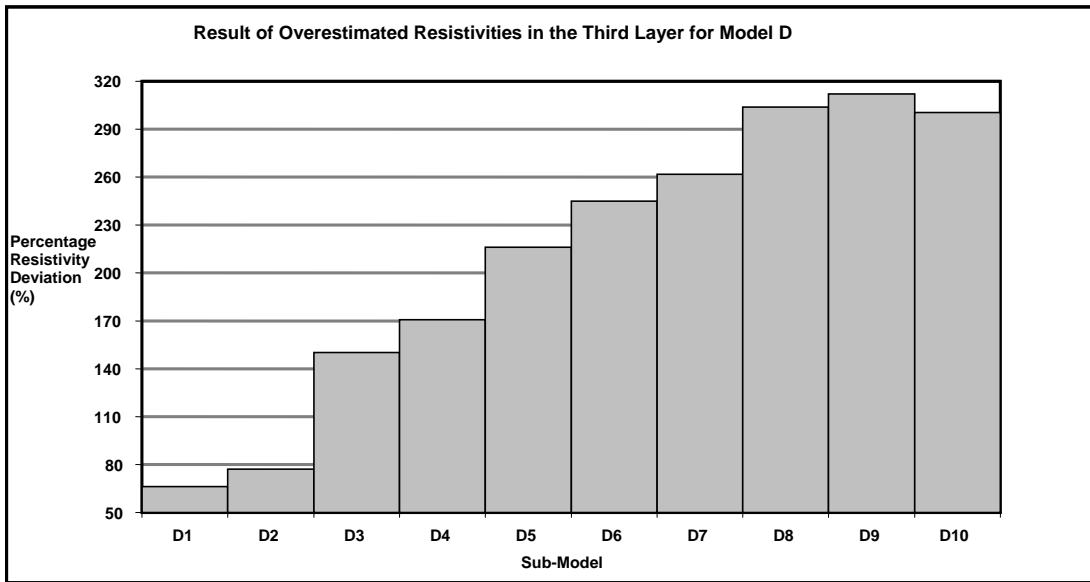


Figure 11(a): Histogram of Percentage Deviation for Third Layer Resistivity for Model D.

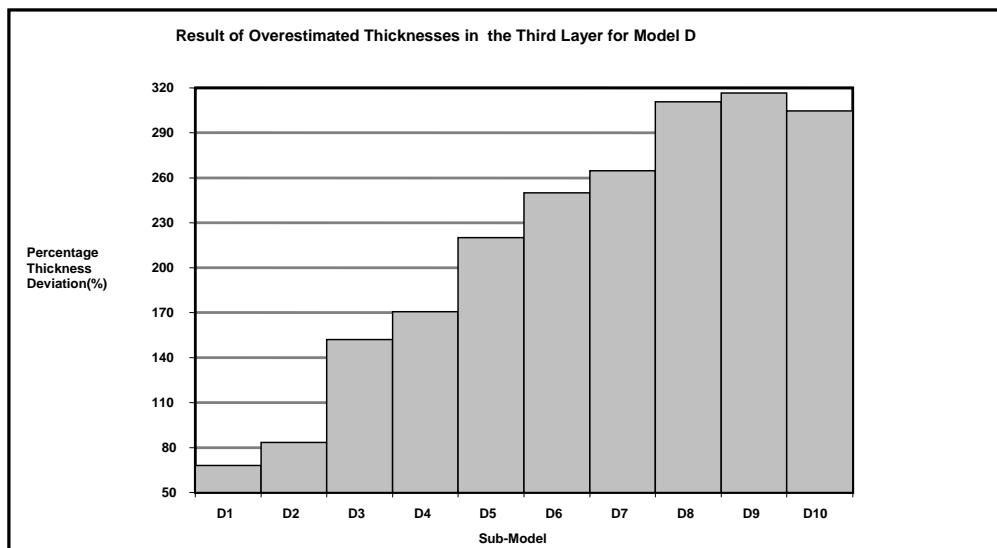


Figure 11(b): Histogram of Percentage Deviation for Third Layer Thickness for Model D.

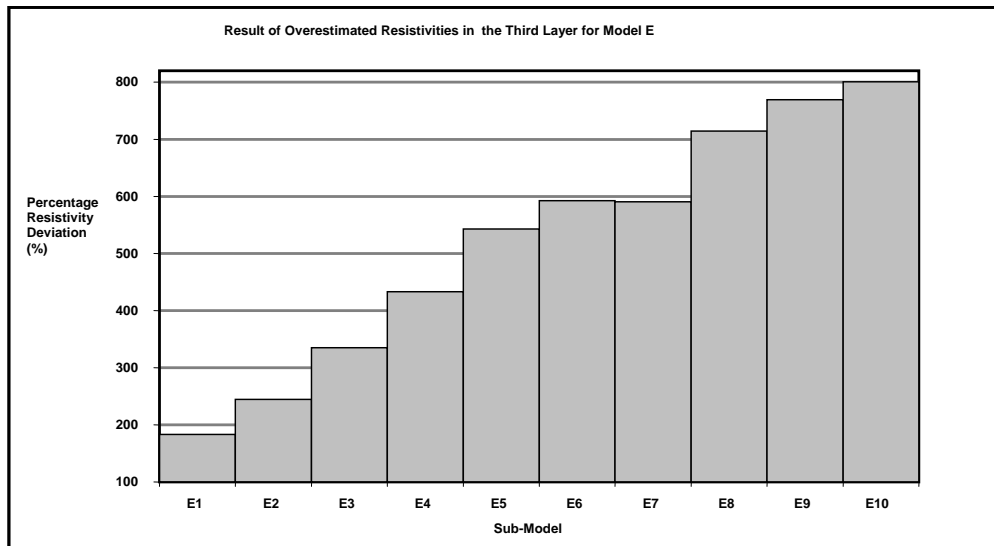


Figure 12(a): Histogram of Percentage Deviation for Third Layer Resistivity for Model E.

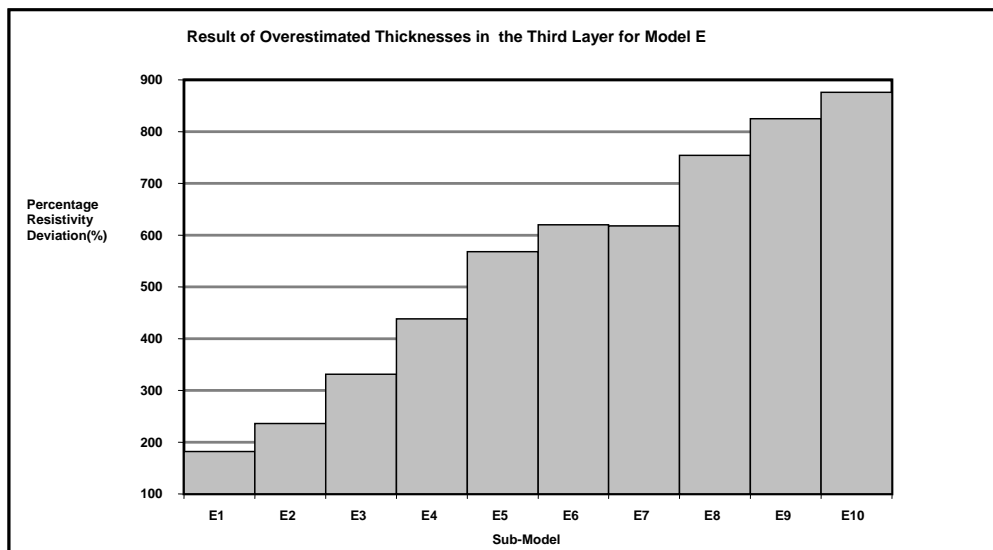


Figure 12(b): Histogram of Percentage Deviation for Third Layer Thickness for Model E.

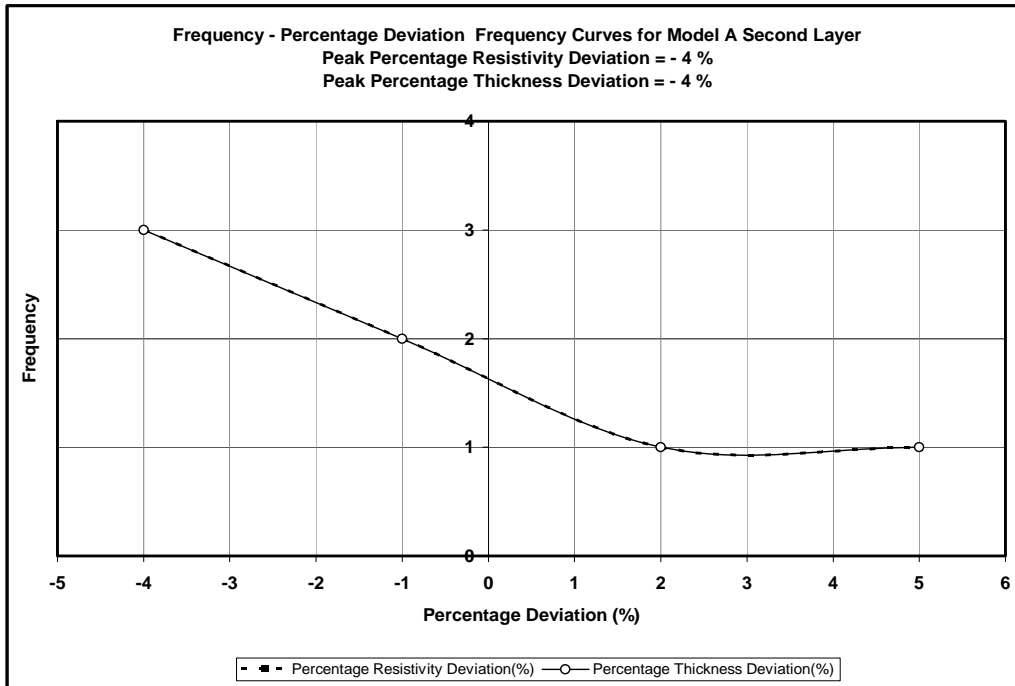


Figure 13(a): Percentage Deviation Frequency Curves for the Second Layer in Model A.

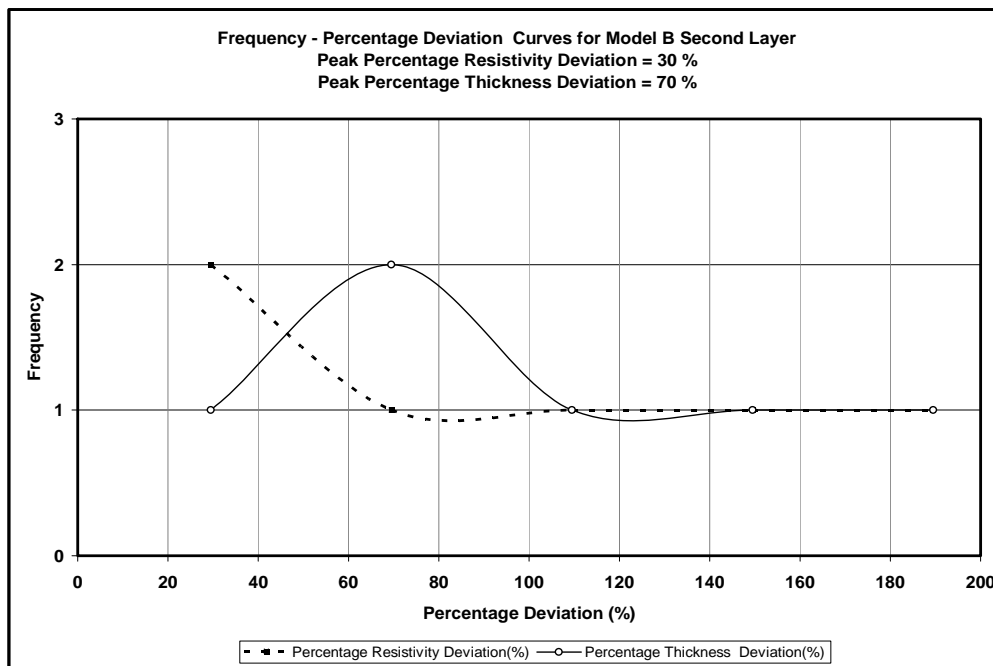


Figure 13(b): Percentage Deviation Frequency Curves for the Second Layer in Model B.

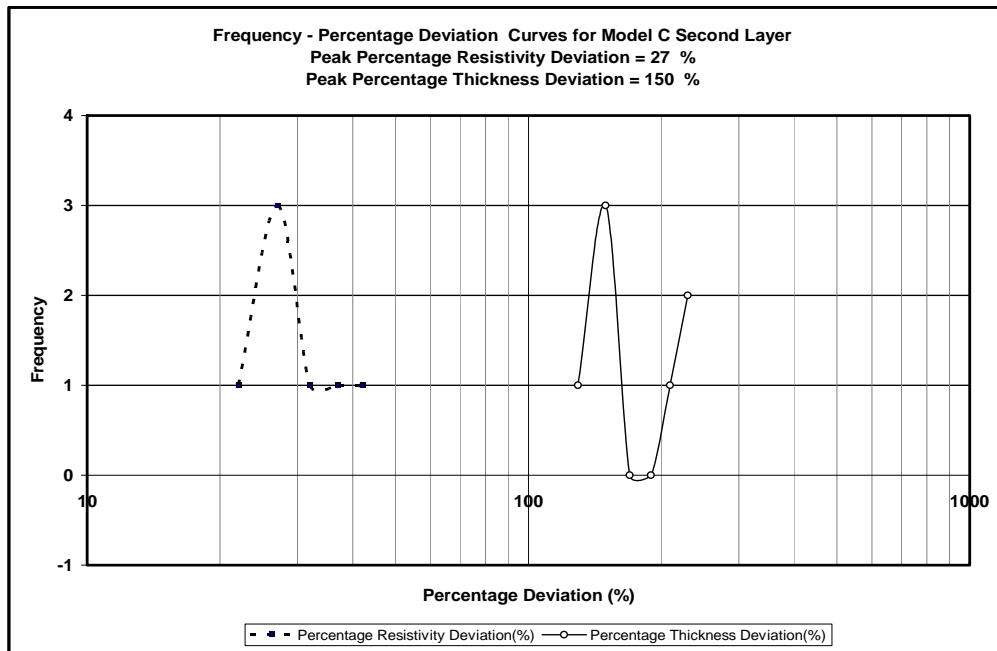


Figure 13(c): Percentage Deviation Frequency Curves for the Second Layer in Model C

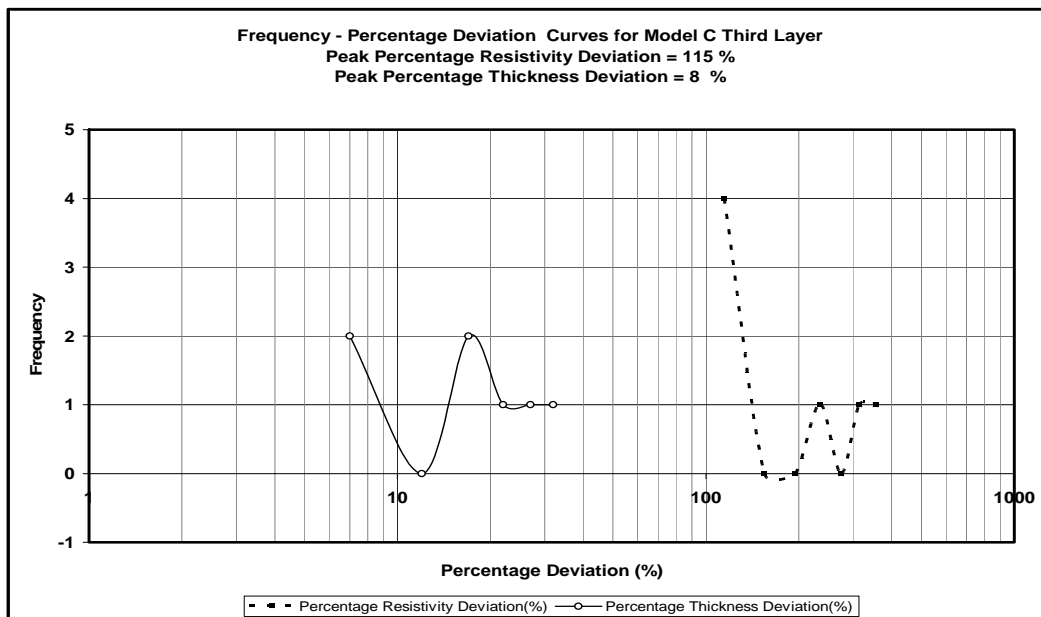


Figure 13(d): Percentage Deviation Frequency Curves for the Third Layer in Model C.

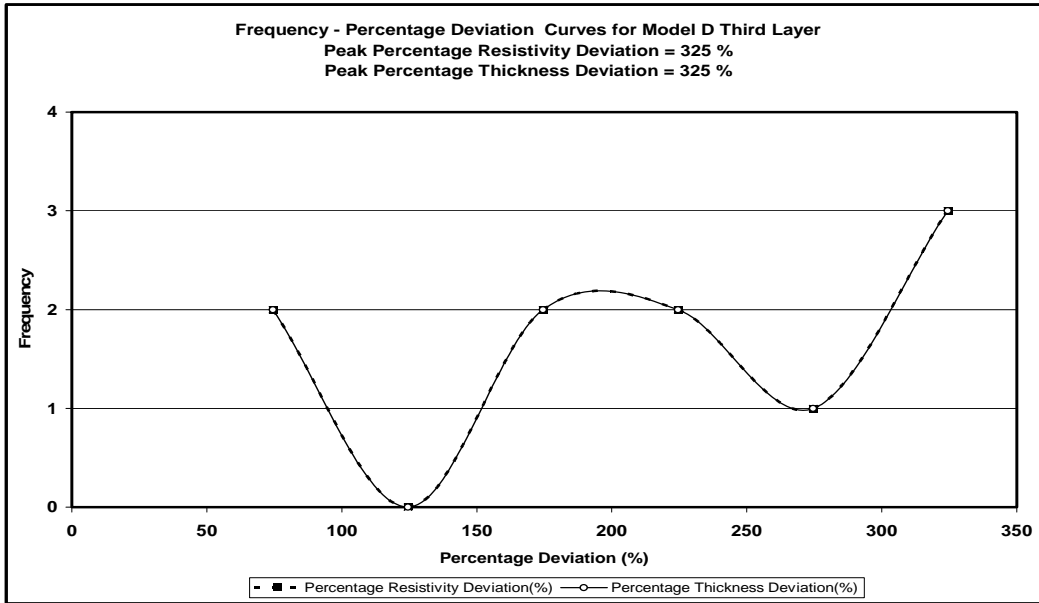


Figure 13(e): Percentage Deviation Frequency Curves for the Third Layer in Model D.

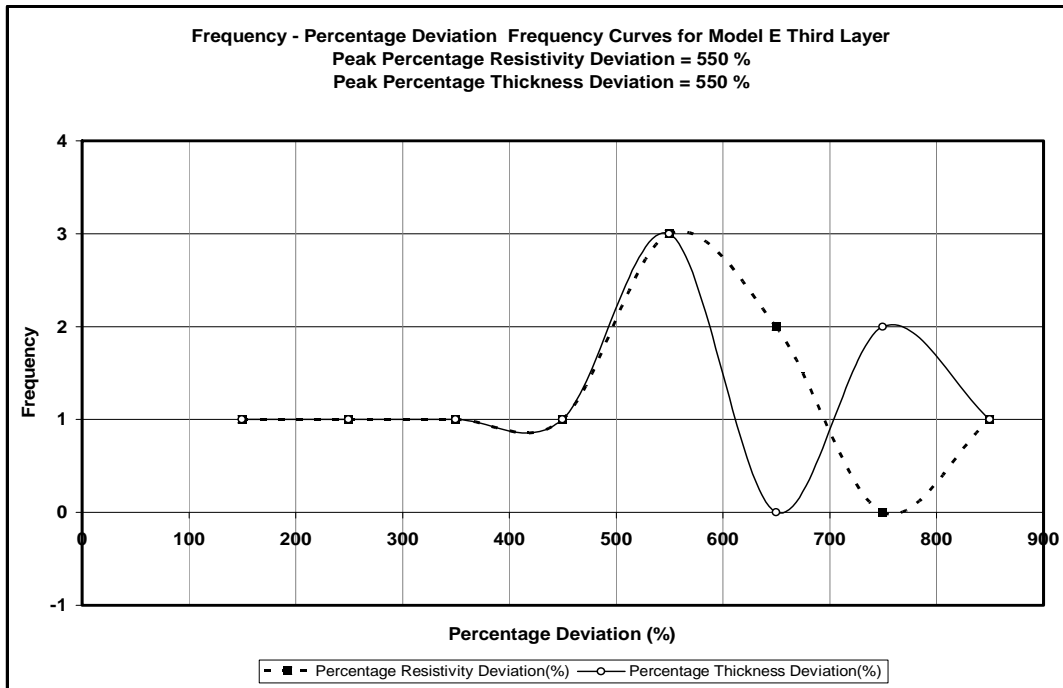


Figure 13(f): Percentage Deviation Frequency Curves for the Third Layer in Model E.

The results of three-layered geoelectric models (models A and B) show that the geoelectric parameters of these models can be accurately determined only when the thickness of the resistive topsoil is thin (less than 2m). Results of four-layered model (model C) with resistive topsoil (first layer) show that the second layer resistivity is slightly overestimated while its thickness is highly overestimated. The third layer thickness is slightly overestimated while its resistivity is highly overestimated. The results from the four-layered models (model D and E) with resistive second layer show that the resistivity and thickness of the third layer can be proportionately highly overestimated.

Generally, the results show that Vertical Electrical Sounding technique could yield abnormally high layer parameters for multiple subsurface layers overlain by a resistive topsoil (upper layer). The degree of overestimation increases with the number of layers and increasing layer thicknesses.

REFERENCES

1. Ademilua, L.O. 2007. "Computer Modelling and Detectability Assessment of the Transition zone in the Basement Complex Terrain of Southwestern Nigeria". Ph.D. Thesis/ Obafemi Awolowo University: Ile-Ife, Nigeria.
2. Ademilua, O.L. and M.O. Olorunfemi. 2008. "An Interactive Software for Schlumberger Theoretical Resistivity Forward Modelling". *Journal of Applied and Environmental Sciences*. University of Louisville, USA. 3(1):1-12.
3. Afolabi, O. and M.O. Olorunfemi. 2004. "Laboratory Modelling of Geoelectric Response of a Leaking Underground Petroleum Storage Tank in Sand Formation". *Global Journal of Geological Sciences*. 2(2):207-220.
4. Aina, A., M.O. Olorunfemi, and J.S. Ojo. 1996. "An Integration of Aeromagnetic and Electrical Resistivity Methods in Dam Site Investigation". *Geophysics*. 61(2): 349-356.

5. Bhattacharya, P.K., and H.P. Patra. 1968. *Direct Current Geo-electric Sounding: Principle and Interpretation*. Elsevier Pub. Co.: Amsterdam, Netherlands. 135.
6. Dooge, J.C. 1967. "The Hydrologic Cycle as a Closed System. In: *Proc. Intern. Hydrol. Symp.* Fort Collins, CO. 98-113.
7. Olorunfemi, M.O. and S.A Fasuyi. 1993. "Aquifer Types and the Geoelectric/Hydrogeologic Characteristics of Parts of the Central Basement Terrain of Nigeria (Niger state)". *Journal of African Earth Sciences*. 16(3):309-317.
8. Olorunfemi, M.O., A.I. Idornigie, H.O. Fagunloye, and O.A. Ogun. 2004. "Assessment of Anomalous Seepage Conditions in the Opa Dam Embankment, Ile-Ife, Southwestern Nigeria". *Global Journal of Geological Sciences*. 2(2):191-198.
9. Vander Velpen, B.P.A. 1988. "RESIST version 1.0". M.Sc. Research Project. ITC: Netherlands.
10. Zohdy, A.A.R., G.P. Eaton, and D.R. Mabey. 1980. "Application of Surface Geophysics to Groundwater Investigations: *Techniques of Water-Resources Investigations of the United States Geological Survey*. 1-3.

SUGGESTED CITATION

Adeniran, A.E., M.O. Olorunfemi, and O.G. Bayowa. 2009. "Computer Model Study of the Effect of Resistive Topsoil on Interpretation Results of Subsurface Geoelectric Layers' Parameters". *Pacific Journal of Science and Technology*. 10(1):635-655.

 [Pacific Journal of Science and Technology](http://www.akamaiuniversity.us/PJST.htm)